

## Aerosol particle properties at a remote tropical rainforest in Borneo

Nur Aleesha Abdullah<sup>a,b</sup>, Mohd Talib Latif<sup>a,\*</sup>, Liew Juneng<sup>a</sup>, Royston Uning<sup>c</sup>,  
Hanashriah Hassan<sup>b</sup>, Azliyana Azhari<sup>d</sup>, Thomas Tuch<sup>e</sup>, Alfred Wiedensohler<sup>e</sup>

<sup>a</sup> Department of Earth Sciences and Environment, Faculty of Science and Technology, Universiti Kebangsaan Malaysia, 43600, Bangi, Selangor, Malaysia

<sup>b</sup> Malaysian Meteorological Department (MetMalaysia), Ministry of Water and Environment, Jalan Sultan, 46667, Petaling Jaya, Selangor, Malaysia

<sup>c</sup> Institute of Oceanography and Environment, Universiti Malaysia Terengganu, 21030, Kuala Nerus, Terengganu, Malaysia

<sup>d</sup> Monash Climate Change Communication Research Node, School of Arts and Social Sciences, Monash University Malaysia, 47500, Bandar Sunway, Selangor Darul Ehsan, Malaysia

<sup>e</sup> Leibniz Institute for Tropospheric Research, 04318, Leipzig, Germany

### ARTICLE INFO

#### Keywords:

PM<sub>10</sub>  
Aerosol particle light absorption  
Aerosol particle light scattering  
Temporal variations  
Wavelet analysis

### ABSTRACT

This paper aims to investigate aerosol particle properties and their seasonal variabilities at a remote tropical forest site. It also attempts to study the relationship between aerosol particles and dynamic atmospheric processes that modulate aerosol variability. Mass concentrations for particles smaller than 10 µm aerodynamic diameter (PM<sub>10</sub>) and optical aerosol particle properties were measured at Danum Valley tropical rainforest in Borneo Island. The particle mass concentrations were measured using a Tapered Element Oscillating Microbalance (TEOM). Measurements of aerosol particle optical properties, i.e., the particle light absorption and scattering coefficients, were conducted using a Multi-Angle Absorption Photometer (MAAP) and nephelometer, respectively. The single scattering albedo (SSA) and scattering Angstrom exponent (SAE) were calculated from the aerosol scattering and absorption coefficients. The results showed that the daily average of PM<sub>10</sub> mass concentrations was 12.3 µg m<sup>-3</sup>, while the particle light absorption coefficients at wavelength 637 nm and scattering coefficients at wavelength 525 nm were reported as 2.7 Mm<sup>-1</sup> and 21.7 Mm<sup>-1</sup>, respectively. The daily average SSA and SAE recorded were 0.89 and 1.44, respectively. The SSA showed no seasonal variations while higher SAE was observed during the dry season due to the influence of biomass burning originating from the southern region of Borneo. The wavelet analysis showed strong intra-seasonal cycles (12–20 and 32–64 days) which suggest the influence of Quasi-BiWeekly (QBW) oscillation and Madden-Julian Oscillation (MJO) on the aerosol variability over the tropics. The analysis also showed seasonal and annual variability bands, generally associated with the dry and wet seasons over the region.

### 1. Introduction

Aerosol consists of solid or liquid particles suspended in the atmosphere in the size range of few nanometres up to 100 µm. These particles are introduced into the atmosphere as primary aerosols, from natural and anthropogenic sources, or as secondary aerosols that are formed by chemical reactions (Birmili et al., 2003; Yin, 2020). Turbulence and movement of air masses through regional or global circulation distribute and disperse aerosols in the atmosphere. Aerosol particles play an important role in the earth's solar radiation budget and water cycle balance, in human health, and in climate change dynamics (IPCC, 2013; Shindell and Faluvegi, 2009). Over the years, the increase in

urbanisation has resulted in heat release, regional pollution, and increased anthropogenic emissions being released into the atmosphere (Liu and Niyogi, 2019). The large variety of aerosols has increased the uncertainty in climate studies and climate models, especially in evaluating global climate change (Eck et al., 2010; Samset et al., 2018). As one of the most variable constituents of the earth's climate, aerosol particles in the atmosphere can alter the climate and radiative balance directly by affecting the transmission of solar radiation through scattering and absorption which can result in either cooling or warming effects on the atmosphere (Cazorla et al., 2013; Myhre et al., 2013; Rama Gopal et al., 2017).

The measurement of aerosol particles is necessary to understand

Peer review under responsibility of Turkish National Committee for Air Pollution Research and Control.

\* Corresponding author.

E-mail address: [talib@ukm.edu.my](mailto:talib@ukm.edu.my) (M.T. Latif).

<https://doi.org/10.1016/j.apr.2022.101383>

Received 30 August 2021; Received in revised form 4 March 2022; Accepted 5 March 2022

Available online 14 March 2022

1309-1042/© 2022 Turkish National Committee for Air Pollution Research and Control. Production and hosting by Elsevier B.V. All rights reserved.

their properties as well as their spatial and temporal variations. Understanding the impact of different aerosol types on regional climate and air quality requires temporal and spatial variation data from the long-term ground-based monitoring of aerosol particles variables (Zhao et al., 2015). Quantitative data on optical aerosol particle properties and their derivatives is necessary to assess the direct effects of aerosols on the earth's radiation balance. Salinas et al. (2009) suggested that the effects of aerosols on the climate are strongly dependent on their optical particle properties. These properties may vary with time and region as aerosol properties that can change in a very short time (Cheng et al., 2006). To date, several extensive studies on optical aerosol particle properties and associated radiative forcing effects at the global scale (Charlson et al., 2016; Chauvigné et al., 2019; Mordas et al., 2015; Pandolfi et al., 2011) and regional scales over the Asian region have been reported (Bibi et al., 2016, 2017; Gong et al., 2015; Iftikhar et al., 2018; Rama Gopal et al., 2017; Sun et al., 2018; Tan et al., 2015; Xin et al., 2016).

The complexities of the radiation effects of aerosol particles still leave much uncertainty for climate change studies, especially over the maritime continent of South-East Asia (SEA) (Reid et al., 2012, 2015; Wang et al., 2013). This region is a major atmospheric heat source that plays an important role in the earth's climate system (Ramage, 1968). Due to the complexity of the land and ocean geography and the surrounding warm ocean waters, the land-sea interaction in this region is extremely complex and difficult to quantify. The complexity of the meteorological and atmospheric scales in this region adds to the global complexity of aerosol systems (Reid et al., 2013). The Danum Valley rainforest, located at the centre of the tropical maritime continent in SEA is a unique site for investigating the effects of aerosols from anthropogenic sources over a naturally clean environment. This site is an ideal location for studying atmospheric interactions, long-range transport of pollutants, and the ability of forests to act as sinks for atmospheric pollutants in a tropical rainforest environment (Fowler et al., 2011; Nomura et al., 2018; Pyle et al., 2011). The clean environment, which is relatively undisturbed and free from any anthropogenic sources, provides an ideal site for baseline studies on aerosol particle properties that can fill the scientific gaps over this region. Therefore, this paper aims to

present a temporal analysis of aerosol particle properties at a remote tropical forest site as well as the seasonal variability. In this investigation, we also discuss the relationships with the synoptic meteorological features and long-range transport scenarios covering annually occurring fire activity in SEA, particularly from Kalimantan, Indonesia. Finally, we also examine the relationship between aerosols and dynamic atmospheric processes that modulate aerosol particle variations.

## 2. Measurements and methods

### 2.1. Site information

In this study, measurements of aerosol particle properties were conducted from May 2010 to April 2015 (PM<sub>10</sub>) and June 2012 to June 2014 (particle light absorption and scattering coefficients), at Danum Valley Global Atmosphere Watch (GAW) station. Danum Valley GAW station (4.96N, 117.6E, approximately 426 m a.s.l.) is located within class one forest in the eastern part of Sabah, Malaysia, on Borneo Island (Fig. 1). Primary tropical rainforests cover this site with widely distributed Dipterocarpaceae as the dominant species, but oil palm fields are also distributed in the north-eastern part of the island (Reynolds et al., 2011). The station is approximately 7 km from the research site of the Danum Valley Field Centre, within the Danum Valley Conservation Area, an area of 438 km<sup>2</sup>. The nearest district of Lahad Datu is located approximately 80 km away in the eastern part of Danum Valley, which is mostly surrounded by oil palm plantations. This site is considered relatively clean and undisturbed, without local anthropogenic aerosol sources, populations, or industries.

Generally, Borneo is influenced by two monsoon seasons throughout the year. The dry season, better known as the southwest monsoon (SW) over this region, lasts from June to August, whereas the wet season, also known as the northeast monsoon (NE), lasts from December to February. Between these monsoon seasons are transition periods known as intermonsoon-I (Inter-I) and intermonsoon-II (Inter-II). To investigate the seasonal variations in PM<sub>10</sub> mass concentrations and optical aerosol particle properties, the data were classified into four monsoonal seasons: NE monsoon (December-January-February/DJF), Inter-I (March-April-

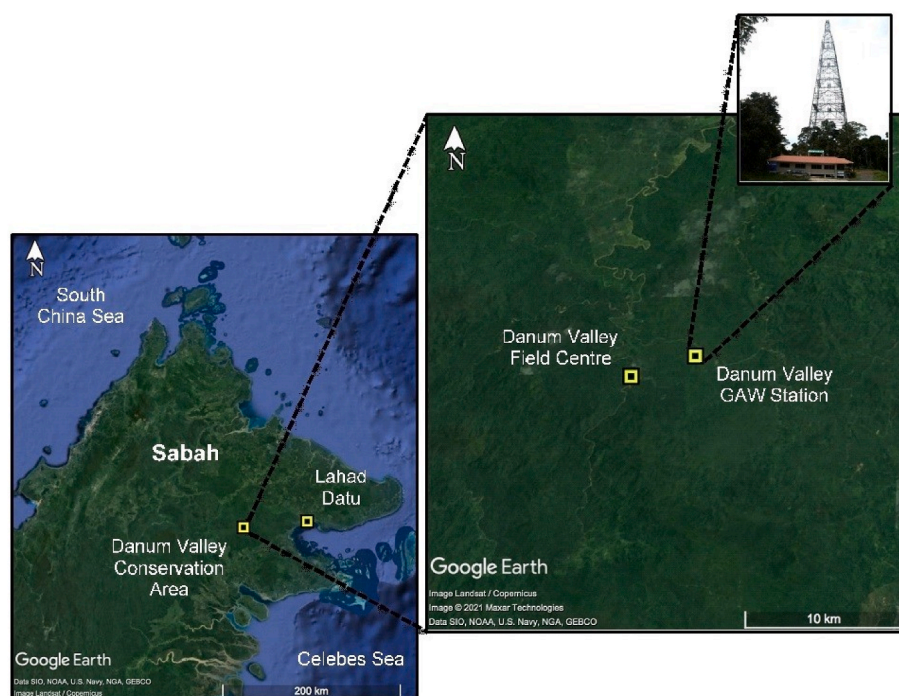


**Fig. 1.** The Danum Valley Global Atmosphere Watch location in Borneo Island and the station with 100 m sampling tower. The detail map in for the study area (.kmz file) is presented in Supplementary 1.

May/MAM), SW monsoon (June-July-August/JJA), and Inter-II (September-October-November/SON).

## 2.2. Aerosol measurements

The aerosol was sampled through a low flow PM<sub>10</sub> inlet, which was located approximately 8 m above the ground on the rooftop of the sampling station. The flow rate drawn through the sample inlet of the TEOM was 16.7 L min<sup>-1</sup> and the temporal measurement was based on 1 min intervals. A Tapered Element Oscillating Microbalance (TEOM) (Rupprecht-Patashnick 1400 ab) was used to measure the ambient particle mass concentration of PM<sub>10</sub>. The measurement of the particle scattering coefficients was conducted with the Aurora 3000 (Ecotech Ptd Ltd), a three-wavelength (450, 525, and 635 nm) integrating nephelometer. This instrument is able to simultaneously measure the particle light scattering and backscattering coefficients with a temporal resolution of 1 min. The flow rate was fixed at 3 L min<sup>-1</sup>.

Aerosol particle light absorption was measured using a Multi-Angle Absorption Photometer (MAAP) (Thermo Inc., Model 5012) (Petzold et al., 2005), operating in parallel with the TEOM and integrating nephelometer. The flow rate in the main inlet line prior to separation into the three different specific paths was 16.7 L min<sup>-1</sup>, and this was maintained for the specific path of samples going to the TEOM. For the MAAP and nephelometer, the flow rate was reduced to 9.0 L min<sup>-1</sup> and 3.0 L min<sup>-1</sup> respectively. The MAAP measured the particle light absorption coefficient at 637 nm (Petzold and Schönlinner, 2004). The TEOM, MAAP, and integrating nephelometer were connected to the same sampling line with the inlet. The sampling site is generally very humid, with a relative humidity of around 90%. To overcome the high humidity in the area and obtain measurements under dry conditions, the inlet was custom-made with two Nafion dryers. In addition, in order to achieve an average relative humidity below 40%, drying of the sampled air for the aerosol system was accomplished using a combination of an air compressor and adsorption dryer. In this study, prior to further analysis, data screening was conducted to filter out invalid data such as data that was captured during routine span and zero checks, calibration, maintenance of instruments and other local influence or work conducted within the vicinity of the station. Apart from that, only data that recorded relative humidity below 40% were considered for further analysis.

## 2.3. Single scattering albedo (SSA) and scattering angstrom exponent (SAE)

This study calculated two additional optical aerosol parameters, namely the scattering Angstrom exponent (SAE) and single scattering albedo (SSA), from the aerosol absorption and scattering coefficients. The SAE, which is an indicator of the average size of the particle population is given by given by:

$$SAE = - \frac{\log\left(\frac{\sigma_{sc}^{\lambda_1}}{\sigma_{sc}^{\lambda_2}}\right)}{\log\left(\frac{\lambda_1}{\lambda_2}\right)} \quad \text{Eq.1}$$

where  $\lambda_1$  and  $\lambda_2$  correspond to wavelengths of 635 nm and 450 nm, respectively. Fine particles associated with biomass burning and urban pollution have SAE values of greater than 2, while larger particles associated with dust and sea salt minerals have SAE values of less than 1 (Schuster et al., 2006). The second aerosol optical parameter is the SSA which is a measure of the aerosol particle scattering strength relative to extinction at the same wavelength. Scattering coefficients at 637 nm were derived from the scattering measurements using the SAE, and the SSA at 637 nm was calculated as:

$$SSA = \frac{\sigma_{sc}}{\sigma_{sc} + \sigma_{abs}} \quad \text{Eq.2}$$

The SSA value can be used an indicator to determine whether the atmospheric particles have a cooling or warming effect on climate. Sulphate, which is a non-absorbing particle, has an SSA value of one, while absorbing particles have a lower SSA value.

Due to the remote location, this GAW station is unmanned and is managed by the Malaysian Meteorological Department. Although the station is equipped with an Automatic Weather Station (AWS) for meteorological parameter observations, the AWS data coverage was very poor due to frequent major breakdowns and connection issues. Thus, as meteorological data was not available, for this study the precipitation rate estimate was obtained from the NASA GPM IMERG (late run) daily with a spatial resolution of 0.1° × 0.1°/10 km. The European Centre for Medium-Range Weather Forecasts (ECMWF) Reanalysis (Era5) with a spatial resolution of 0.25° × 0.25° was used to provide the daily average wind data at 925 hPa. The NOAA hotspots information and data were retrieved from the ASEAN Specialised Meteorological Centre's website (ASMC). The details of tropical cyclones in the western north Pacific issued by the Japan Meteorological Agency (JMA) were used to provide an insight into the high-pressure systems that may affect the atmospheric conditions over the sampling site.

To identify possible aerosol sources, back trajectories were simulated using the Hybrid Single-Particle Lagrangian Integrated Trajectory Model (HYSPPLIT) version 4.9, developed and maintained by the National Oceanic and Atmospheric Administration (NOAA)'s Air Resource Laboratory (ARL) (Draxler, 1999). Using meteorological data obtained from the NCEP Final Analysis (FNL) archive, the analysis runs were for a 72-h backward kinematics trajectory from Danum Valley station at 500 m above ground level (a.g.l.). The 72-h back trajectory is an ideal period to identify the movement of air masses which originated from pollutant sources over the region such as Kalimantan and the South China Sea. According to Nomura et al. (2018), the height of the stable and convective boundary layer at Danum Valley can reach up to 2400 m during the daytime, depending on the weather conditions in the area. Thus, the 500 m height of the trajectories is sufficient to identify the path of the chemical species and particulates at the Danum Valley monitoring station.

Wavelet analysis can be used to reveal oscillatory or periodicity behaviour in a dataset, as detailed in Torrence and Compo (1998). In this study, wavelet analysis was computed using the WaveletComp package in the R language program. The Morlet 'mother' wavelet function was used to compute the wavelet power spectrum, and the method is extensively detailed in the WaveletComp Guide handbook (Roesch and Schmidbauer, 2018). The wavelet power spectrum is given by:

$$\varphi(t) = \pi^{-1/4} e^{-i\omega t} e^{-t^2/2} \quad \text{Eq.3}$$

where  $\varphi(t)$  is the wavelet value at non-dimensional time,  $t$  and  $\omega$  is the non-dimensional frequency. Wavelet analysis has been applied in many signal processing applications including atmospheric aerosol data analysis in (Barik et al., 2020; Beegum et al., 2009; Kabanov et al., 2011; Wang et al., 2020).

## 3. Results and discussion

### 3.1. Overview and variations of aerosol optical properties

Table 1 presents a statistical summary of the daily average PM<sub>10</sub> concentrations and aerosol optical properties measured during the entire study period. From the table, it can be seen that there is significant day-to-day variability in PM<sub>10</sub> mass concentrations, particle light absorption and scattering coefficients. The daily average values of PM<sub>10</sub> mass concentration ranged between 3.0 and 47.9 μg m<sup>-3</sup> with an average and standard deviation of 12.3 ± 5.00 μg m<sup>-3</sup> for the entire period. The daily average absorption coefficient values at 637 nm ranged from 0.560 to 15.4 Mm<sup>-1</sup> with an average and standard deviation of 2.76 ± 1.68

**Table 1**

Summary of daily aerosol concentrations for PM<sub>10</sub> mass concentrations (May 2010 to April 2015), particle light absorption and scattering coefficients (June 2012 to June 2014) measured in Danum Valley.

Parameter	Min	Max	Avg ± Stdev	Q1	Median	Q3
PM <sub>10</sub> ( $\mu\text{g m}^{-3}$ )	3.04	47.9	12.3 ± 5.00	9.07	11.0	14.2
$\sigma_{\text{ap}}$ ( $\text{Mm}^{-1}$ )	0.560	15.4	2.76 ± 1.68	1.73	2.39	3.21
$\sigma_{\text{sp}}$ ( $\text{Mm}^{-1}$ )	3.34	161	21.7 ± 18.9	10.1	15.6	27.3
SSA <sub>637 nm</sub>	0.734	0.963	0.890 ± 0.03	0.862	0.896	0.920
SAE <sub>450-635 nm</sub>	0.530	2.32	1.44 ± 0.350	1.07	1.48	1.75

Note: Min = Minimum, Max = Maximum, Avg = Average, Stdev = Standard Deviation, Q1 = Quartile 1, Q3 = Quartile 3,  $\sigma_{\text{ap}}$  = particle light absorption coefficients at 637 nm wavelength,  $\sigma_{\text{sp}}$  = particle light scattering coefficients at 525 nm wavelength, SSA = single scattering albedo, SAE = scattering Angstrom exponent.

$\text{Mm}^{-1}$ . Meanwhile, the scattering coefficient at 525 nm varied from 3.34 to 161  $\text{Mm}^{-1}$  with an average of  $21.7 \pm 18.9 \text{ Mm}^{-1}$ .

Being located deep in the remote tropical rainforest, the average 24-h concentration of PM<sub>10</sub> ( $12.3 \mu\text{g m}^{-3}$ ) indicated the concentration of a remote site within tropical forest. Compared to Jerantut, a background site in Peninsular Malaysia, the daily average of PM<sub>10</sub> concentration over Danum Valley was also much lower, with Jerantut recording a daily average of  $37.9 \mu\text{g m}^{-3}$  (Latif et al., 2014). The nearest town of Tawau, 80 km away from Danum Valley in the eastern part of Borneo, recorded a daily average PM<sub>10</sub> concentration of  $47.6 \mu\text{g m}^{-3}$  which was measured using the beta attenuation method (BAM, Met One Instruments, Inc) from 2002 to 2012 (Mohtar, 2017). While Danum Valley had a daily average of  $2.7 \text{ Mm}^{-1}$  for particle light absorption coefficient, a study in the Amazon, Brazil over a primary tropical forest site by Rizzo et al. (2013), recorded a daily average of  $2.3 \text{ Mm}^{-1}$ . However, both tropical forest sites recorded an equivalent daily average of  $21 \text{ Mm}^{-1}$  for the particle light scattering coefficient. This is to be expected as the main sources for scattering aerosol are mostly from biogenic sources and

forest metabolism (Chauvigné et al., 2019; Pyle et al., 2011).

The temporal variations of daily average values of PM<sub>10</sub> mass concentrations, particle light absorption coefficients at 637 nm, scattering coefficients at 525 nm and SSA are shown in Fig. 2(a), 2(b), 2(c) and 2(d), respectively. Daily average values for all measurements were calculated from hourly values. Throughout the entire measurement period, there were a few significant extreme values observed with all three instruments. From May 2010 to April 2015, among the highest values of daily PM<sub>10</sub> mass concentrations were recorded on August 26, 2011, September 13, 2012, and October 4, 2014, while particle light absorption and particle scattering coefficients were observed to be the highest on September 13, 2012. This maximum occurred almost annually during the dry season over the region between July and October. Within this time frame, extreme values compared to normal can be observed and are primarily associated with the haze episodes experienced over the region (Latif et al., 2018). This period with dry weather provides ideal conditions for initiating and maintaining burning with high fractional smouldering emissions, especially over the region with a large area of tropical peatland (Reid et al., 2012). One of the main contributing factors has been attributed to transboundary transportation of biomass burning over Borneo, particularly in Kalimantan, Indonesia. During this period, an excessive number of hotspots identified by satellite observation have been reported over Kalimantan and attributed to the dry season over the region. Apart from that, local burning to clear land for agricultural purposes also contributes to the haze conditions.

Fig. 3 shows wind and precipitation data for September 13, 2012 that correspond to one of the days that observed the highest daily PM<sub>10</sub> mass concentrations, particle light absorption coefficients and scattering coefficients. As mentioned previously, satellite data showed a high number of hotspots detected on that particular day over the Kalimantan region located in the southern part of Borneo. With the wind blowing from the southwest direction, it transported the biomass burning emissions from the southern region towards the northern region of Borneo. The transport of biomass burning emissions reached the measurement site, and

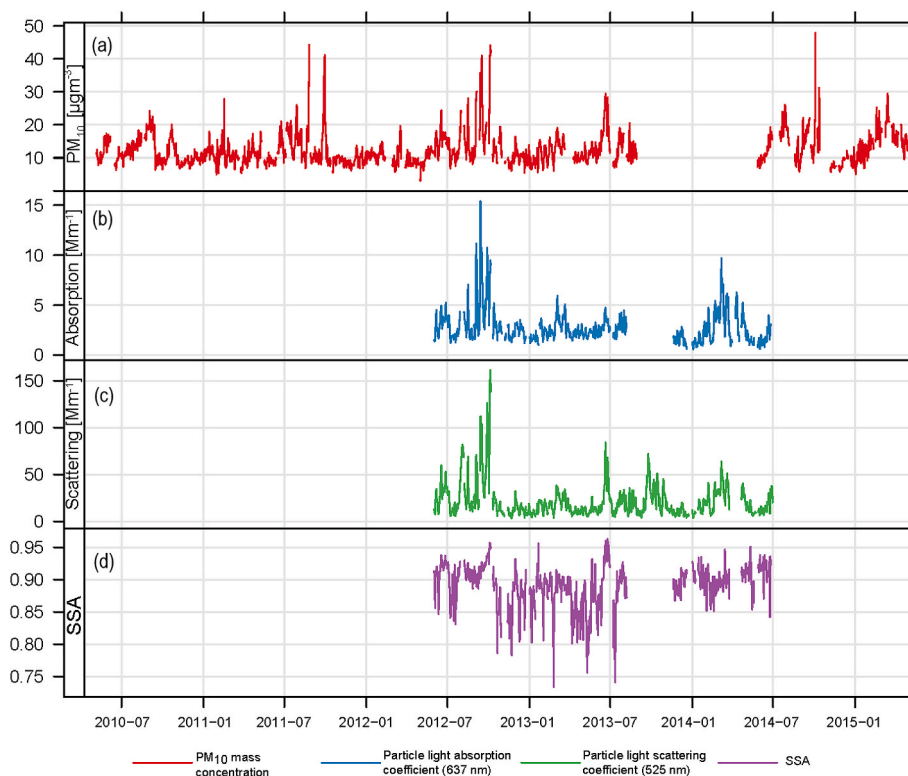


**Fig. 2.** Daily mean of (a) PM<sub>10</sub> mass concentrations, (b) particle light absorption coefficients at 637 nm, (c) particle light scattering coefficients at 525 nm and (d) SSA in Danum Valley.

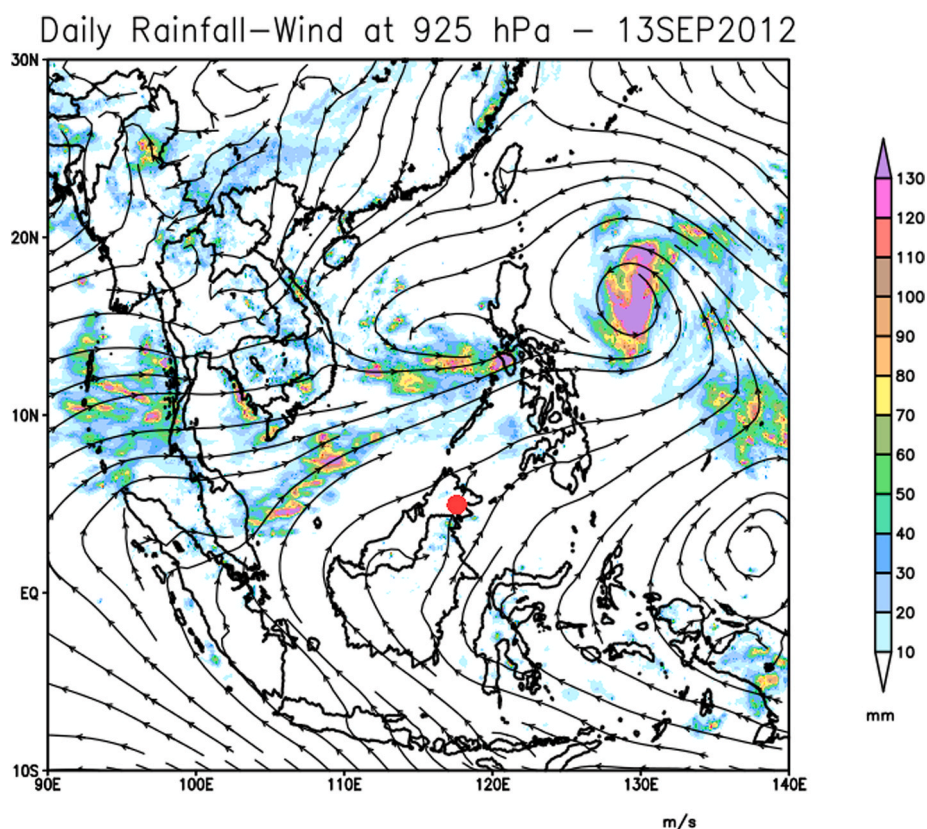


Fig. 3. The daily wind at 925 hPa and precipitation on September 13, 2012, which had the highest recorded daily PM<sub>10</sub> mass concentrations, particle light absorption and scattering coefficients during the measurement period.

the data clearly shows that these emissions were recorded in Danum Valley. Meteorological factors, including typhoons and wind patterns, contribute to major peat-burning pollution events and transport (Hansen et al., 2019; Wang et al., 2013). The smoke transport during these particular events was also enhanced by typhoons that developed over the northwest Pacific and South China Sea (SCS), as shown in Fig. 3. Japan Meteorological Agency (JMA) issued three typhoon warnings, namely Typhoon Nanmadol (August 2011), Super Typhoon Sanba (September 2012), and Super Typhoon Phanfone (October 2014), which coincided with several of the observations of the highest daily mean for all three aerosol parameters. The impacts on the aerosol variations due to the strengthening of southwesterly winds over the equatorial region and the formation of cyclonic circulation have also been reported (Hansen et al., 2019; Juneng et al., 2011).

As shown in Fig. 2(a–c), the daily aerosol average data demonstrated a similar trend among all three aerosol parameters during the respective period. Analysis of the relationship between parameters is tabulated in Table 2. The analysis shows a strong positive correlation between particle light absorption and scattering coefficients, with the highest

correlation of  $r = 0.87$ , followed by PM<sub>10</sub> mass concentrations and scattering coefficients with  $r = 0.84$ . While the relationship between PM<sub>10</sub> mass concentrations and particle light absorption coefficients shows the least correlation with  $r = 0.77$ , it still exhibits a strong correlation between the two parameters. For a clearer graphical representation of this relationship, the aerosol data obtained at minute intervals were used to calculate the monthly averaged values.

### 3.2. Diurnal variations

The study of diurnal variability can offer more understanding of the fundamental processes that govern the evolution of aerosol properties in Danum Valley, including particle formation mechanisms and emissions. Furthermore, a detailed examination of diurnal trends could help to identify local and regional sources. In Danum Valley, the diurnal pattern of PM<sub>10</sub> mass concentrations showed that the concentrations started to increase from sunrise at around 06:00 and reached the highest concentrations of  $16.5 \mu\text{g m}^{-3}$  sometime around 08:00 (Fig. 4). The increase seen during the early morning was partly due to the sources coming from morning activities within the vicinity of the area. However, the PM<sub>10</sub> mass concentrations started to decrease after 2 h and remained stable until late afternoon. The concentrations began to decline gradually at 17:00 and continued to decline throughout the night, reaching a minimum at midnight and remaining below  $10 \mu\text{g m}^{-3}$  until the early morning hours. The stability of the boundary layer influences the aerosol particle mass and number concentrations; it becomes more active during the day due to increased solar heating and is more stable at night as a result of surface cooling. After sunrise, the boundary layer often thickens due to increased solar heating, resulting in the mixing of clean air from above with the polluted air below. As a result, the aerosol density gradually decreases as aerosols are transported from the surface to a higher level in the atmosphere (Rama Gopal et al., 2017).

Table 2  
Correlation matrix between the three parameters observed from June 2012 to June 2014.

Parameter	PM <sub>10</sub> mass concentration	Absorption coefficient <sub>s<sub>637nm</sub></sub>	Scattering coefficient <sub>s<sub>525nm</sub></sub>
PM <sub>10</sub> mass concentrations	1		
Absorption coefficient <sub>s<sub>637nm</sub></sub>	0.77**	1	
Scattering coefficient <sub>s<sub>525nm</sub></sub>	0.84**	0.87**	1

\*\*Correlation is significant at the 0.01 level (2-tailed).

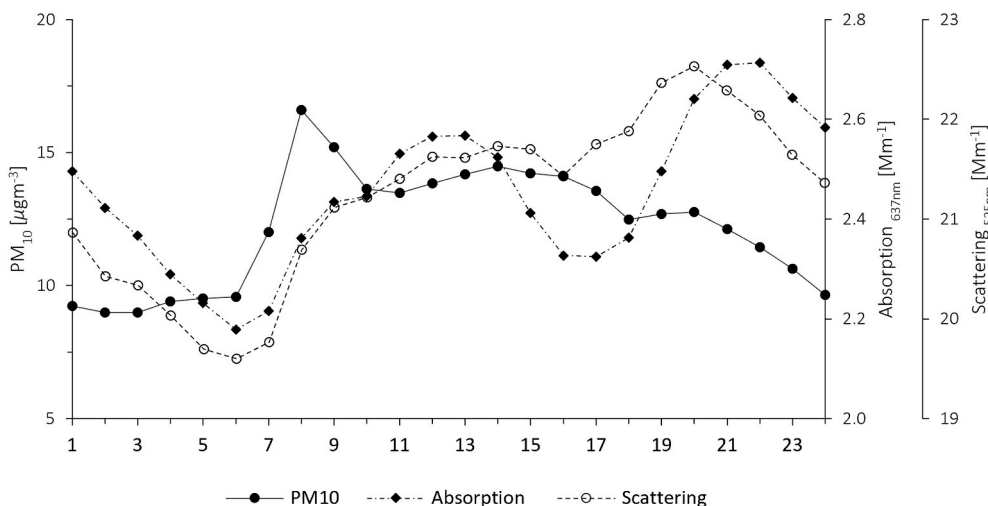


Fig. 4. Diurnal pattern (local time) of PM<sub>10</sub> mass concentrations, particle light absorption and scattering coefficients.

Contrary to PM<sub>10</sub> mass concentrations, the particle light absorption coefficients exhibited two maxima and two minima within a day. The latter reached the first peak at 12:00, while the second peak occurred at 21:00. The diurnal patterns for this coefficient also clearly demonstrated that the second peak was greater than the first. After the second maxima which are due to lower mixing height, the absorption coefficient began to continuously decrease until reaching the first minima at 06:00 the following morning. It also had the second minima around 17:00 in the late afternoon before starting to increase to the highest maxima of the day. Like PM<sub>10</sub> mass concentrations, scattering coefficients began to increase gradually after sunrise and reached a maximum at 20:00. Subsequently, the scattering coefficient decreased steadily throughout the night, reaching a minimum at around 06:00 in the morning. This shows that the particle light scattering coefficient is greater during the day compared to at night. Several studies have shown that the steady increase in the scattering coefficient during the day may be attributed to the photochemical formation of biogenic secondary organic aerosols and increase in larger size scattering aerosol types in the forest area (Chen et al., 2009; Rama Gopal et al., 2017; Rizzo et al., 2013). While the particle light absorption keeps increasing during the night, the decrease in particle light scattering might indicate that the particulate matter that caused the light scattering was most likely photochemically produced. The diurnal patterns show that the site was affected by primary

emissions, secondary formations, and the physical mixing of different air masses within and around the valley.

### 3.3. Monthly variations

Fig. 5 shows the temporal monthly average variations of all three aerosol particle parameters measured in Danum Valley from May 2010 to April 2015 (PM<sub>10</sub>) and June 2012 to June 2014 (particle light absorption and scattering coefficients). From this figure, it can be seen that the monthly average values clearly showed similar trends among parameters with significant peaks and minima across temporal scales. PM<sub>10</sub> mass concentrations recorded monthly average values of between 7.16 and 21.7 µgm<sup>-3</sup> with the minimum value recorded in November 2014 and the maximum in September 2012. Similarly, the particle light absorption coefficients also recorded the highest monthly average of 5.88 Mm<sup>-1</sup> in September 2012, while May 2014 recorded the lowest monthly average of 1.45 Mm<sup>-1</sup>. The monthly average for particle light scattering coefficients varied between 9.78 and 57.2 Mm<sup>-1</sup>, with the minimum value recorded in November 2012 and the maximum in September 2012. Generally, all three aerosol particle parameters exhibited higher values during the September and October periods, the region's dry season.

In September 2012, all three aerosol particle parameters showed the

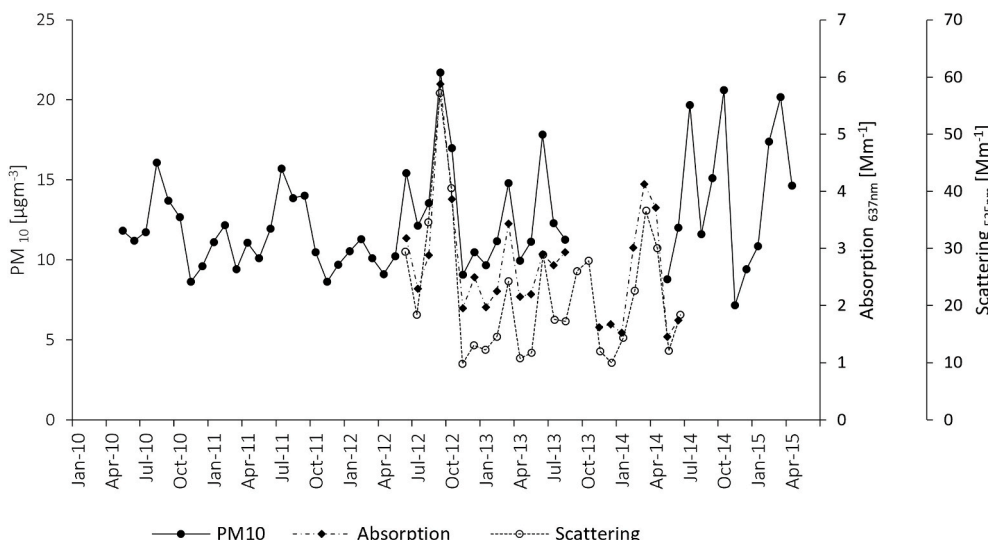


Fig. 5. Monthly variations of PM<sub>10</sub> mass concentrations, particle light absorption and scattering coefficients.

highest values at the sampling site. A study by Reddington et al. (2014) on the role of vegetation and peat fires in particulate air pollution in SEA showed that the most intense burning occurred annually in September and October. High values of PM<sub>10</sub> mass concentrations and particle light absorption coefficients can be attributed to the transboundary transport of aerosol particles from biomass burning in Borneo's southwest and southern regions (Juneng et al., 2009, 2011; Koplitz et al., 2018; Kusumaningtyas et al., 2016; Mahmud, 2013). Based on the records, 5525 burning hotspots were detected in September 2012, with the highest numbers recorded in Kalimantan for September within the five years of the study period. According to Reid et al. (2012), a large-scale aerosol environment was modulated by the Madden-Julian Oscillation (MJO) and its associated tropical cyclone activity over SCS. As a result, September 2012 saw an MJO dry phase which created ideal dry conditions for biomass burning activities (Reid et al., 2016).

In 2014, the region in south SEA experienced an intense MJO dry phase and drought. Due to the prolonged dry season, higher burning activity over the world's largest tropical peatland in that year revealed a few significant peaks. October 2014 saw the highest number of hotspots recorded in 2014, with 16,860 burning hotspots detected over Borneo. Generally, the three aerosol particle parameters demonstrated a similar monthly pattern throughout the measurement period. However, on several occasions, a particular parameter was more dominant in terms of magnitude. For instance, particle light scattering coefficients showed greater magnitude than particle light absorption coefficients during August to September 2012 and June 2013. A study conducted by Rizzo et al. (2013) over a primary tropical forest in Amazonia found that particle scattering was much more enhanced, especially during the dry season. They detailed the results and remarked that the air masses that arrived at the measurement sites were a mixture of smoke plumes from various fire stages and ages. According to Reid et al. (2005), deforestation fires can smoulder for days, producing particles with high emission factor rates but low black carbon content. This will reduce the particle light absorption and increase the particle light scattering of the

original plume (Kusumaningtyas et al., 2016; Reid et al., 2012). Additionally, particle light scattering also increases with plume age, due to physical and chemical atmospheric processes that contribute to particle size and mass growth, and gas-to-particle exchanges. A study by Capes et al. (2008) also reported that in situ measurements of biomass burning plumes showed that black carbon content typically reduced by 10–50% during the transition from fresh smoke to regional haze due to dilution with cleaner background air. Therefore, particle light scattering and absorption coefficients can vary significantly, depending on the plume characteristics and atmospheric conditions (Rizzo et al., 2013). Throughout the period, there were times when the particle light absorption coefficients were dominant over the particle light scattering coefficients. Burning activities over Borneo occurred less frequently during the wet or rainy seasons (Kusumaningtyas et al., 2016). Local aerosol sources, particularly anthropogenic aerosol transferred from the surrounding area to the sampling site in the forest, were most likely the primary sources that influence the higher particle light absorption coefficients. This may explain why particle light absorption predominated over particle light scattering from aged smoke plumes during the wet season, especially from November to February.

### 3.4. Seasonal variations of aerosol properties

In this section, the seasonal averages for all aerosol particle data were calculated using hourly data, as shown in Table 3. While there were variations between years, the data revealed a significant seasonal pattern throughout the years. JJA had the highest seasonal average PM<sub>10</sub> value of 13.7 ± 4.81 μgm<sup>-3</sup>, followed by SON (12.8 ± 7.12 μgm<sup>-3</sup>) and MAM (11.5 ± 3.71 μgm<sup>-3</sup>). In terms of particle light absorption coefficients, the transition monsoon Inter-II recorded the highest seasonal average of 3.87 ± 2.97 Mm<sup>-1</sup> for SON and 2.85 ± 1.50 Mm<sup>-1</sup> for the MAM period while JJA averaged 2.80 ± 0.98 Mm<sup>-1</sup>. SON had the greatest seasonal average values of particle light scattering coefficients at 29.1 ± 19.5 Mm<sup>-1</sup>, followed by JJA (24.2 ± 16.6 Mm<sup>-1</sup>)

**Table 3**  
Annual seasonal variations of PM<sub>10</sub> mass concentrations, particle light absorption and scattering coefficients.

	PM <sub>10</sub> (μgm <sup>-3</sup> )			Absorption Coeff. <sub>637nm</sub> (Mm <sup>-1</sup> )			Scattering Coeff. <sub>525nm</sub> (Mm <sup>-1</sup> )		
	Q1	Median	Q3	Q1	Median	Q3	Q1	Median	Q3
DJF 2010	9.12	10.60	12.18						
DJF 2011	9.08	10.44	11.38						
DJF 2012	8.62	10.40	12.38	1.61	2.14	2.94	7.46	12.29	19.55
DJF 2013	n.a	n.a	n.a	1.08	1.69	3.30	6.97	12.92	26.07
DJF 2014	9.01	11.83	14.18						
DJF mean	10.96 ± 3.11			2.15 ± 0.95			14.43 ± 7.76		
MAM 2011	8.77	10.00	11.69						
MAM 2012	8.11	9.46	11.50						
MAM 2013	9.70	11.36	13.05	1.82	2.38	3.32	8.74	13.32	25.17
MAM 2014	8.52	8.68	9.34	1.33	2.55	5.24	9.77	22.02	40.54
MAM 2015	14.32	16.0	19.61						
MAM mean	11.46 ± 3.71			2.85 ± 1.50			19.17 ± 11.82		
JJA 2010	10.71	12.64	15.27						
JJA 2011	10.07	13.02	17.41						
JJA 2012	10.61	12.81	16.12	1.69	2.63	3.85	10.78	21.45	43.77
JJA 2013	9.98	12.69	16.82	2.09	2.79	3.64	9.87	18.27	32.33
JJA 2014	9.44	13.63	17.46						
JJA mean	13.76 ± 4.81			2.80 ± 0.98			24.16 ± 16.62		
SON 2010	8.34	9.82	14.55						
SON 2011	8.37	9.41	10.60						
SON 2012	9.43	12.88	18.23	1.78	2.97	7.31	10.73	22.7	52.55
SON 2013	n.a	n.a	n.a	1.11	1.63	2.01	8.53	14.66	38.99
SON 2014	7.73	11.74	17.17						
SON mean	12.84 ± 7.12			3.87 ± 2.97			29.14 ± 19.45		

Note: DJF = Northeast monsoon, MAM = Intermonsoon-I, JJA = Southwest monsoon, SON = Intermonsoon-II, Q1 = Quartile 1, Q3 = Quartile 3, n.a = data not available.

and MAM ( $19.2 \pm 11.8 \text{ Mm}^{-1}$ ). The DJF season had the lowest seasonal averages for  $\text{PM}_{10}$  mass concentrations, particle light absorption coefficients, and particle light scattering coefficients at  $11.0 \pm 3.11 \mu\text{gm}^{-3}$ ,  $2.15 \pm 0.950 \text{ Mm}^{-1}$  and  $14.4 \pm 7.76 \text{ Mm}^{-1}$ , respectively. Given that the data distribution was widely spread with extreme values for significant events, median values for year-to-year seasonal variations were considered a better representation of the data set.

Year-to-year seasonal variations showed that MAM in 2015 had the highest median  $\text{PM}_{10}$  mass concentrations of  $16.0 \mu\text{gm}^{-3}$ . From Table 3, it can be seen that  $\text{PM}_{10}$  mass concentrations and particle light absorptions coefficients generally recorded a higher median during JJA annually. However, based on the records, very dry weather and severe haze over the region during 2015 (Department-of-Environment, 2015; McBride et al., 2015) saw the median for  $\text{PM}_{10}$  mass concentrations during MAM 2015 pass the higher JJA (2010–2014) record. With the dry spell coupled with light and variable low-level winds during this period, these conditions created more favourable conditions for particulates to remain longer in the atmosphere (Hansen et al., 2019). The particle light scattering median in SON 2012 also demonstrated the highest recorded season. During this dry season with a transitioning wind direction period, massive burning of forest, crops, and land clearing over the region is common and transboundary haze episodes are expected to occur annually in the region (Reid et al., 2012; Wang et al., 2013; Yin, 2020). Many farmers use the slash-and-burn approach to clear vegetation for palm oil, pulp, and paper crops. As mentioned, aged smoke plumes when transported will contribute more to the particle light scattering. Precipitation intensity and the strength of biomass burning sources are contributing factors to the variations in the aerosol. The particle light scattering coefficients of particles rose significantly when biomass burning particles were present during this monsoon. This is due to the greater concentration of fine mode particles during the dry season, which scatter light more effectively than the coarse mode dominated biogenic particles during the wet season (Rizzo et al., 2013). DJF marks the onset of the NE monsoon season, during which the region experiences the rainy season with abundant rainfall and prevailing winds from the northeast of SCS. Generally, burning is less prevalent, and this season

also saw the lowest  $\text{PM}_{10}$  mass concentrations, particle light absorption and scattering coefficients.

Fig. 6 depicts the 72-h mean percentage air mass back trajectory over Borneo calculated using HYSPLIT for September 13, 2012, a significant haze episode case study with one of the highest daily averages recorded in Danum Valley. In this case, the back trajectory showed that most of the air mass originated from the southwest of Danum Valley with the highest percentage of air mass (37%) originating from Sarawak, Malaysia. Sarawak, located in the southwest of Danum Valley and northern Kalimantan, is also one of the contributing areas for the deterioration of air quality over the northern Borneo region. This state is home to most of Malaysia's peatlands, about 70% (~1.6 Mha) of the total 2.6 Mha of peatland in Malaysia (Melling, 2016). Usually, peat fires generate thick smoke in the atmosphere during dry spells. Rampant burning by local farmers in peatland areas in Sarawak and peatland development for agricultural purposes contribute to the severe haze conditions.

In Sarawak, deterioration in air quality due to small-scale burning is often reported in the northern division, particularly over Mukah, Bintulu, Sibul and Miri. During the September 2012 scenario, burning was most prevalent in September and early October. While the burning and meteorology were typical during this time, the fire activities were strongly modulated in Sumatra and Borneo by the MJO and SW monsoon flows. As the season progressed, fire activities consistently increased in the eastern islands, which is the characteristic of regional burning activity (Reid et al., 2016). Additionally, the higher daily values recorded over Danum Valley during this period were also attributed to the smoke transported from Central and East Kalimantan (31%), Sulawesi (22%), with the least being from northern Borneo and the Philippines (9%).

In this study, the average mass scattering efficiency and mass absorption efficiency of the aerosol particles are calculated as the ratio of particle light scattering coefficients and absorption coefficients to the  $\text{PM}_{10}$  mass concentrations, respectively. For the two years measured, the average mass scattering efficiency was  $1.45 \pm 0.550 \text{ m}^2\text{g}^{-1}$  and was in the range  $0.540\text{--}3.66 \text{ m}^2\text{g}^{-1}$ . Higher scattering efficiency can be

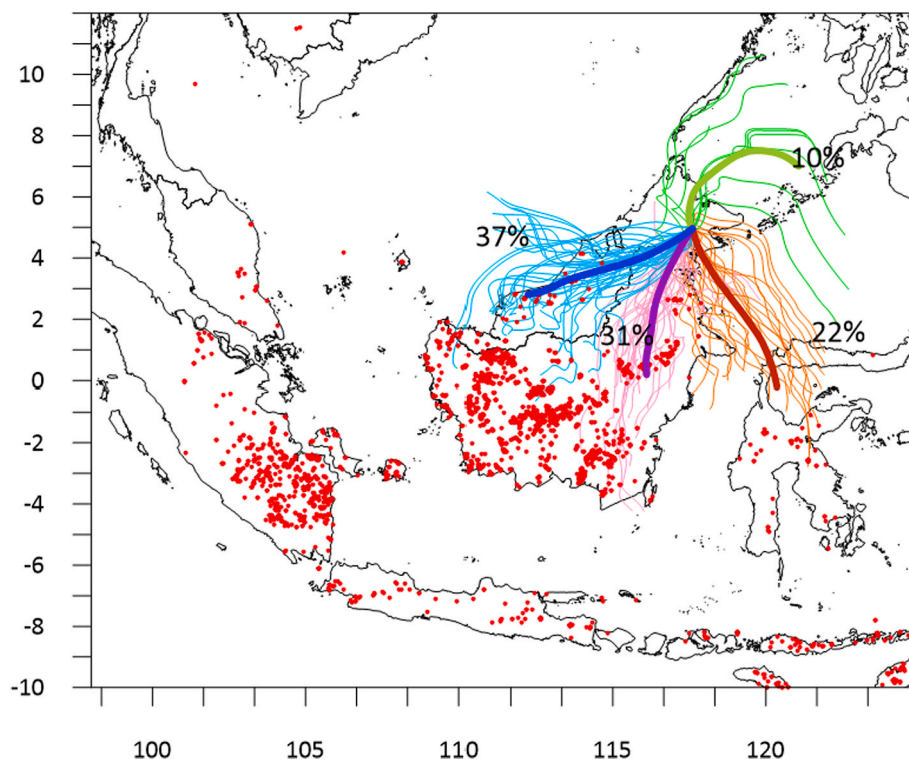


Fig. 6. 72-h mean air mass back trajectories (%) estimated using HYSPLIT for September 13, 2012, with different line colours representing each trajectory group.

observed during the dry season (SON) which can be attributed to fine particles released from biomass burning activities, while the rainy season revealed the lowest values. The average mass absorption efficiency ranged from 0.10 to 0.43 with an average of  $0.210 \pm 0.050 \text{ m}^2\text{g}^{-1}$  with no significant seasonal variations, except several short periods within the burning season.

### 3.5. Single scattering albedo (SSA) and scattering angstrom exponent (SAE)

The SSA and SAE values over Danum Valley are tabulated in Table 4. From the analysis, the overall average and median for SSA were  $0.89 \pm 0.03$ , ranged between 0.73 and 0.96 (Fig. 2(d)). Generally, absorbing particles will have lower SSA values, and in situ measurements of dry aerosols show that urban aerosols and fresh biomass burning will have SSA values of 0.80–0.98 and 0.72–0.88, respectively (Anderson, 2003; Magi et al., 2003). Although there was a seasonal variation in the particle light absorption and scattering coefficients, the SSA values at this site did not show any seasonal variations ( $\text{SSA} = 0.88\text{--}0.89$ ).

For the SAE measurements, the results showed that the overall average and median values were  $1.44 \pm 0.34$  and 1.48, respectively. The average SAE in this remote Borneo forest was slightly lower than an Amazonian forest site (1.59) (Rizzo et al., 2013). Between seasons, the highest SAE was observed during the MAM (1.73) while DJF had the lowest SAE (1.22). During the dry season, JJA and SON recorded average SAE values of 1.43 and 1.40, respectively.

During the Inter-I dry spell experienced over the Borneo region with light and variable winds, favourable conditions are experienced for more biomass burning activities locally or in the neighbouring country. With the weakening of the prevailing winds, fine particles from biomass burning are more likely to be confined to and remain longer in the atmosphere (Rizzo et al., 2013; Schuster et al., 2006). For comparison, the average SAE during Inter-I was approximately 28% greater than during the NE monsoon, the rainy season. During the NE monsoon, heavy rainfall may help wash out and remove particles from the atmosphere (Rama Gopal et al., 2017).

### 3.6. Periodicity characteristics of the aerosol data

The periodic oscillations of  $\text{PM}_{10}$  mass concentrations, particle light absorption and scattering coefficients at different time scales using wavelet analysis are shown in Fig. 7. From the analysis, most of the power was concentrated within the bands of 8–64 days and 64–128 days (Fig. 7(a–c)), which are suggested to be associated with intra-seasonal and inter-seasonal oscillations, respectively. The 8–64 day band was obvious in the power spectrum, especially during the JJA and SON periods which are associated with dry seasons. It was also suggested that there was a modulation of 30–60 days in the aerosol concentrations through rainfall variation, with the intra-seasonal signature strongest

**Table 4**  
Annual seasonal variations of single scattering albedo ( $\text{SSA}_{637\text{nm}}$ ) and scattering Angstrom exponent ( $\text{SAE}_{450-635\text{nm}}$ ).

Parameter	Min	Max	Avg $\pm$ Stdev	Q1	Median	Q3
<i>Single Scattering Albedo<sub>637nm</sub></i>						
Overall	0.73	0.96	$0.89 \pm 0.03$	0.86	0.89	0.92
MAM	0.75	0.95	$0.88 \pm 0.03$	0.85	0.89	0.91
JJA	0.74	0.96	$0.89 \pm 0.04$	0.87	0.90	0.92
SON	0.78	0.95	$0.89 \pm 0.04$	0.84	0.90	0.92
DJF	0.73	0.96	$0.88 \pm 0.03$	0.86	0.89	0.91
<i>Scattering Angstrom Exponent<sub>450-635nm</sub></i>						
Overall	0.53	2.32	$1.44 \pm 0.34$	1.07	1.48	1.75
MAM	0.82	2.25	$1.73 \pm 0.28$	1.49	1.72	2.01
JJA	0.47	1.92	$1.43 \pm 0.28$	1.22	1.49	1.66
SON	0.64	2.32	$1.40 \pm 0.34$	1.07	1.41	1.66
DJF	0.53	2.29	$1.22 \pm 0.33$	0.91	1.23	1.58

during the summer season (Juneng et al., 2009).

Fig. 7(d–f) shows the average wavelet power for all three aerosol parameters at a 0.05 confidence level. Generally, from the intra-seasonal scale, it can be observed that the highest peak in the average wavelet power for  $\text{PM}_{10}$  mass concentrations occurred on 12-, 20- and 32-day cycles. A similar peak can also be observed for the aerosol particle light absorption and scattering coefficients with 12-, 16-, 32- and 44-day periodicities in the average wavelet power. Previous studies have demonstrated that the convective system over the maritime continent in the tropics is strongly influenced by quasi-biweekly (QBW) oscillation, with a 10–20-day fluctuation (Wen and Zhang, 2008). Since rainfall processes substantially influence aerosol mass concentrations, the less than three weeks (20 days) periodicity characteristics embedded in the signal are found to be associated with the dry and wet spells, which are modulated by the QBW oscillation (Juneng et al., 2009).

Apart from QBW oscillation, the MJO is also considered to be one of the key drivers governing the aerosol variations over the tropics and has been well documented in many studies (Reid et al., 2012, 2015). A study by Tian et al. (2008) using several global satellite products indicated the possibility that the MJO modulates aerosol variability. Over the Western Pacific Ocean, an active MJO convection region, the study found a strong relationship between annual cycles and inter-annual variability with the intra-seasonal aerosol variations. The wavelet analysis for Danum Valley showed a strong power level within the 32–64-day band, and the average wavelet power revealed a significant peak at periodicities of 32 and 44 days. These results might indicate an MJO influence on the intra-seasonal variability in the aerosol concentrations (Ragsdale et al., 2013). In a study over Peninsular Malaysia, Koplitz et al. (2018) also suggested that the MJO probably plays a significant role in modulating the intra-seasonal variations of meteorological conditions which have a substantial impact on aerosol variability.

Seasonal variation characteristics can also be reflected in the wavelet analysis for all three sets of aerosol particle data. There were clear high-frequency bands within the 128–256-day and 256–512-day bands, which are generally associated with the dry and wet seasons over the region and the annual cycle, respectively. The annual periodicity was present throughout the study period. The peak in average wavelet power showed a cycle of about one year (~370 days) for all the aerosol particle parameters.

## 4. Conclusions

The results from this study found the average values of daily  $\text{PM}_{10}$  mass concentrations to be  $12.3 \mu\text{g m}^{-3}$ . The particle light absorption coefficients at a wavelength of 637 nm and particle light scattering coefficients at a wavelength of 525 nm were reported as  $2.7 \text{ Mm}^{-1}$  and  $21.7 \text{ Mm}^{-1}$ , respectively. The diurnal cycle for  $\text{PM}_{10}$  mass concentrations and particle light scattering coefficients exhibited one maxima peak while the particle light absorption coefficients demonstrated two maxima and minima during the entire day. The monsoonal season also found to influence the variations of aerosol particle properties whereby the southwest monsoon and transitions between monsoons showed higher  $\text{PM}_{10}$  mass concentrations, particle light absorption and scattering coefficients than the northeast monsoon. The seasonal variations are due to the aerosol sources and synoptic factors, which play significant roles in varying aerosol particle properties. The average daily SSA and SAE recorded were 0.89 and 1.44, respectively. SSA did not show any seasonal variations while SAE demonstrate higher SAE during the intermonsoon and dry season. The aerosol particle measurement at this site have showed the influence of biomass burning episode originating from the southern region of Borneo. The wavelet analysis showed periodicity characteristics in the aerosol particle data at this remote site. There was a strong intra-seasonal cycle (12–20 days and 32–64 days) which suggests the influence of QBW oscillation and MJO on the aerosol variability over the tropics. The study also showed seasonal (128–256 days) and annual (256–512 days) characteristic bands that were

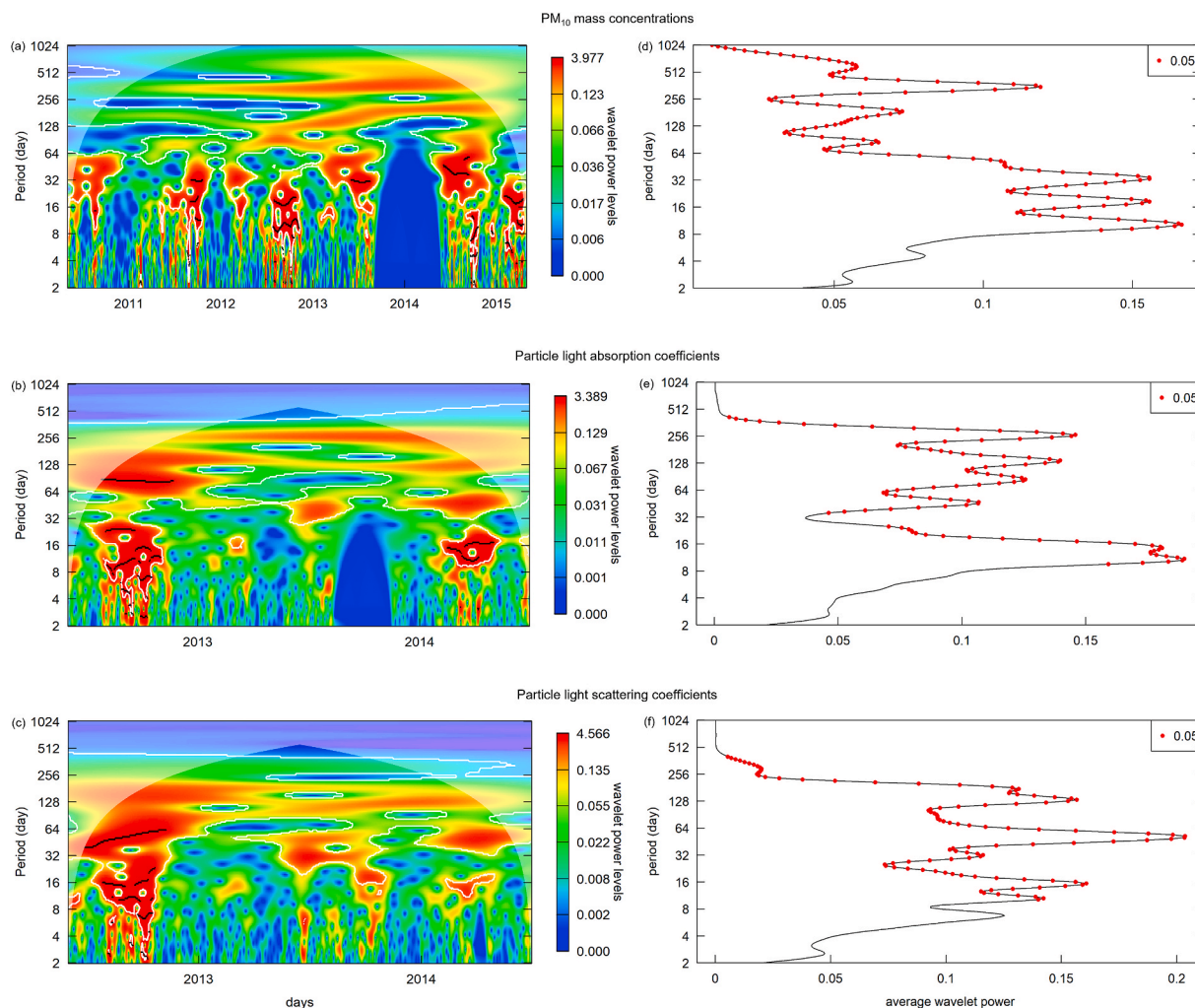


Fig. 7. Averaged wavelet power spectrum of  $PM_{10}$  mass concentrations (May 2010 to April 2015), particle light absorption and scattering coefficients (June 2012 to June 2014) for Danum Valley.

generally associated with the dry and wet seasons, and the annual cycle over the region, respectively. This study is essential as a reference for any other studies in background conditions and a comparison for other studies in urban and industrial background conditions. However, the limitation of this study is the high humidity condition at the observation site. Due to this condition, particles' morphology and mixing states may have changed significantly compared to freshly emitted particles. Thus, the findings in this study may be only applicable to tropical regions. In addition, more detailed studies to determine the dominant aerosol component at this site for both biomass burning and non-biomass burning periods are recommended for future studies.

#### Credit author statement

Nur Aleesha Abdullah: Conceptualization, Writing – original draft. Mohd Talib Latif: Writing – review & editing, Supervision. Liew Juneng: Writing – review & editing, Supervision. Royston Uning: Writing – review & editing. Hanashriah Hassan: Writing – review & editing. Thomas Tuch: Writing – review & editing. Alfred Wiedensohler: Writing – review & editing, Supervision.

#### Declaration of competing interest

The authors declare that they have no known competing financial interests or personal relationships that could have appeared to influence

the work reported in this paper.

#### Acknowledgement

The authors would like to thank the Malaysian Meteorological Department for providing the aerosols data and to Leibniz Institute for Tropospheric Research for instrumentation and technical support for the aerosol measurements at the Danum Valley GAW station. The acknowledgement also goes to R Foundation for providing free access to R software and *openair* package (Carslaw and Ropkins, 2012). The main author also wishes to thank the Malaysian Public Service Department for the study leave scholarship. Special thanks to Dr Rose Norman for proofreading this manuscript. This project is partially funded by Research University Grant by Universiti Kebangsaan Malaysia (DIP-2019-006).

#### Appendix A. Supplementary data

Supplementary data associated with this article can be found, in the online version, at <https://doi.org/10.1016/j.apr.2022.101383>.

#### References

- Anderson, T.L., 2003. Variability of aerosol optical properties derived from in situ aircraft measurements during ACE-Asia. *J. Geophys. Res.* 108 (D23) <https://doi.org/10.1029/2002jd003247>. ACE 15-11-ACE 15-19.

- Barik, G., Acharya, P., Maiti, A., Gayen, B.K., Bar, S., Sarkar, A., 2020. A synergy of linear model and wavelet analysis towards space-time characterization of aerosol optical depth (AOD) during pre-monsoon season (2007–2016) over Indian sub-continent. *J. Atmos. Sol. Terr. Phys.* 211 <https://doi.org/10.1016/j.jastp.2020.105478>.
- Beegum, S.N., Krishna Moorthy, K., Babu, S.S., Reddy, R.R., Gopal, K.R., 2009. Large scale modulations of spectral aerosol optical depths by atmospheric planetary waves. *Geophys. Res. Lett.* 36 (3) <https://doi.org/10.1029/2008gl036509> n/a-n/a.
- Bibi, S., Alam, K., Chishtie, F., Bibi, H., 2016. Characterization of absorbing aerosol types using ground and satellites based observations over an urban environment. *Atmos. Environ.* 150, 126–135. <https://doi.org/10.1016/j.atmosenv.2016.11.052>.
- Bibi, S., Alam, K., Chishtie, F., Bibi, H., Rahman, S., 2017. Observations of black carbon aerosols characteristics over an urban environment: radiative forcing and related implications. *Sci. Total Environ.* 603–604, 319–329. <https://doi.org/10.1016/j.scitotenv.2017.06.082>.
- Birmili, W., Berresheim, H., Plass-Dülmer, C., Elste, T., Gilge, S., Wiedensohler, A., Uhrner, U., 2003. The Hohenpeissenberg aerosol formation experiment (HAFEX): a long-term study including size-resolved aerosol, H<sub>2</sub>SO<sub>4</sub>, OH, and monoterpenes measurements. *Atmos. Chem. Phys.* 3, 361–376.
- IPCC, Boucher, O., Randall, D., Artaxo, P., Bretherton, C., Feingold, G., Forster, P., Kerminen, V.-M., Kondo, Y., Liao, H., Lohmann, U., Rasch, P., Satheesh, S.K., Sherwood, S., Stevens, B., Zhang, X.Y., 2013. 2013: clouds and aerosols. In: Stocker, T.F., Qin, D., Plattner, G.-K., Tignor, M., Allen, S.K., Boschung, J., Nauels, A., Xia, Y., Bex, V., Midgley, P.M. (Eds.), *Climate Change 2013: the Physical Science Basis. Contribution of Working Group I to the Fifth Assessment Report of the Intergovernmental Panel on Climate Change*.
- Capes, G., Johnson, B., McFiggans, G., Williams, P.I., Haywood, J., Coe, H., 2008. Aging of biomass burning aerosols over West Africa: aircraft measurements of chemical composition, microphysical properties, and emission ratios. *J. Geophys. Res.* 113 <https://doi.org/10.1029/2008jd009845>.
- Carslaw, D.C., Ropkins, K., 2012. Openair — an R package for air quality data analysis. *Environ. Model. Software* 27–28, 52–61. <https://doi.org/10.1016/j.envsoft.2011.09.008>.
- Cazorla, A., Bahadur, R., Suski, K.J., Cahill, J.F., Chand, D., Schmid, B., Prather, K.A., 2013. Relating aerosol absorption due to soot, organic carbon, and dust to emission sources determined from in-situ chemical measurements. *Atmos. Chem. Phys.* 13 (18), 9337–9350. <https://doi.org/10.5194/acp-13-9337-2013>.
- Charlson, R.J., Porch, W.M., Waggoner, A.P., Ahlquist, N.C., 2016. Background aerosol light scattering characteristics: nephelometric observations at Mauna Loa Observatory compared with results at other remote locations. *Tellus* 26 (3), 345–360. <https://doi.org/10.3402/tellusa.v26i3.9840>.
- Chauvigné, A., Aliaga, D., Sellegri, K., Montoux, N., Krejci, R., Močnik, G., Laj, P., 2019. Biomass burning and urban emission impacts in the Andes Cordillera region based on in situ measurements from the Chacaltaya observatory, Bolivia (5240 m a.s.l.). *Atmos. Chem. Phys.* 19 (23), 14805–14824. <https://doi.org/10.5194/acp-19-14805-2019>.
- Chen, Q., Farmer, D.K., Schneider, J., Zorn, S.R., Heald, C.L., Karl, T.G., Martin, S.T., 2009. Mass spectral characterization of submicron biogenic organic particles in the Amazon Basin. *Geophys. Res. Lett.* 36 (20) <https://doi.org/10.1029/2009gl039880>.
- Cheng, T., Wang, H., Xu, Y., Li, H., Tian, L., 2006. Climatology of aerosol optical properties in northern China. *Atmos. Environ.* 40 (8), 1495–1509. <https://doi.org/10.1016/j.atmosenv.2005.10.047>.
- Department-of-Environment, 2015. Chronology of Haze Episodes in Malaysia. Retrieved from <https://www.doe.gov.my/portals/1/en/info-umum/info-kuaiti-udara/kronologi-episod-jerebu-di-malaysia/319123>.
- Draxler, R.R., 1999. *HYSPPLIT4 User's Guide*. NOAA Tech. Memo. ERL ARL-230. Silver Spring (MD).
- Eck, T.F., Holben, B.N., Sinyuk, A., Pinker, R.T., Goloub, P., Chen, H., Xia, X., 2010. Climatological aspects of the optical properties of fine/coarse mode aerosol mixtures. *J. Geophys. Res.* 115 (D19) <https://doi.org/10.1029/2010jd014002>.
- Fowler, D., Nemitz, E., Misztal, P., Di Marco, C., Skiba, U., Ryder, J., Hewitt, C.N., 2011. Effects of land use on surface-atmosphere exchanges of trace gases and energy in Borneo: comparing fluxes over oil palm plantations and a rainforest. *Philos. Trans. R. Soc. Lond. B Biol. Sci.* 366 (1582), 3196–3209. <https://doi.org/10.1098/rstb.2011.0055>.
- Gong, W., Zhang, M., Han, G., Ma, X., Zhu, Z., 2015. An investigation of aerosol scattering and absorption properties in wuhan, Central China. *Atmosphere* 6 (4), 503–520. <https://doi.org/10.3390/atmos6040503>.
- Hansen, A.B., Witham, C.S., Chong, W.M., Kendall, E., Chew, B.N., Gan, C., Lee, S.-Y., 2019. Haze in Singapore – source attribution of biomass burning PM10 from Southeast Asia. *Atmos. Chem. Phys.* 19 (8), 5363–5385. <https://doi.org/10.5194/acp-19-5363-2019>.
- Ifitkhar, M., Alam, K., Soroshian, A., Syed, W.A., Bibi, S., Bibi, H., 2018. Contrasting aerosol optical and radiative properties between dust and urban haze episodes in megacities of Pakistan. *Atmos. Environ.* 173, 157–172. <https://doi.org/10.1016/j.atmosenv.2017.11.011>.
- Juneng, L., Latif, M.T., Tangang, F.T., Mansor, H., 2009. Spatio-temporal characteristics of PM10 concentration across Malaysia. *Atmos. Environ.* 43 (30), 4584–4594. <https://doi.org/10.1016/j.atmosenv.2009.06.018>.
- Juneng, L., Latif, M.T., Tangang, F., 2011. Factors influencing the variations of PM10 aerosol dust in Klang Valley, Malaysia during the summer. *Atmos. Environ.* 45 (26), 4370–4378. <https://doi.org/10.1016/j.atmosenv.2011.05.045>.
- Kabanov, D.M., Kurbangaliev, T.R., Rasskazhikova, T.M., Sakerin, S.M., Khutorova, O. G., 2011. The influence of synoptic factors on variations of atmospheric aerosol optical depth under Siberian conditions. *Atmospheric and Oceanic Optics* 24 (6), 543–553. <https://doi.org/10.1134/s102485601106008x>.
- Kopplitz, S.N., Mickley, L.J., Jacob, D.J., Marlier, M.E., DeFries, R.S., Gaveau, D.L.A., Myers, S.S., 2018. Role of the madden-julian oscillation in the transport of smoke from Sumatra to the Malay peninsula during severe non-el niño haze events. *J. Geophys. Res. Atmos.* 123 (11), 6282–6294. <https://doi.org/10.1029/2018jd028533>.
- Kusumaningtyas, S.D.A., Aldrian, E., Rahman, M.A., Sopaheluwakan, A., 2016. Aerosol properties in central kalimantan due to peatland fire. *Aerosol Air Qual. Res.* 16 (11), 2757–2767. <https://doi.org/10.4209/aaqr.2015.07.0451>.
- Latif, M.T., Dominick, D., Ahamad, F., Khan, M.F., Juneng, L., Hamzah, F.M., Nadzir, M. S., 2014. Long term assessment of air quality from a background station on the Malaysian Peninsula. *Sci. Total Environ.* 482–483, 336–348. <https://doi.org/10.1016/j.scitotenv.2014.02.132>.
- Latif, M.T., Othman, M., Idris, N., Juneng, L., Abdullah, A.M., Hamzah, W.P., Jaafar, A. B., 2018. Impact of regional haze towards air quality in Malaysia: a review. *Atmos. Environ.* 177, 28–44. <https://doi.org/10.1016/j.atmosenv.2018.01.002>.
- Liu, J., Niyogi, D., 2019. Meta-analysis of urbanization impact on rainfall modification. *Sci. Rep.* 9 (1), 7301. <https://doi.org/10.1038/s41598-019-42494-2>.
- Magi, B.I., Hobbs, P.V., Schmid, B., Redemann, J., 2003. Vertical profiles of light scattering, light absorption, and single scattering albedo during the dry, biomass burning season in southern Africa and comparisons of in situ and remote sensing measurements of aerosol optical depths. *J. Geophys. Res. Atmos.* 108 (D13), 8504. <https://doi.org/10.1029/2002jd002361>.
- Mahmud, M., 2013. Assessment of atmospheric impacts of biomass open burning in Kalimantan, Borneo during 2004. *Atmos. Environ.* 78, 242–249. <https://doi.org/10.1016/j.atmosenv.2012.03.019>.
- Mcbride, J.L., Sahany, S., Hassim, M.E.E., Nguyen, C.M., Lim, S.-Y., Rahmat, R., Cheong, W.-K., 2015. The 2014 record dry spell at Singapore: an intertropical convergence zone (ITCZ) drought. *Bull. Am. Meteorol. Soc.* 96, S126–S130.
- Melling, L., 2016. Peatland in Malaysia. In: *Tropical Peatland Ecosystems*, pp. 59–73.
- Mohtar, A.A.A., 2017. *Impact of Meteorological Factors on Long-Term Air Pollutants in Malaysia*. (Master Dissertation). Universiti Kebangsaan Malaysia, Bangi, Selangor.
- Mordas, G., Prokopciuk, N., Byčenkienė, S., Andrijauskienė, J., Ulevičius, V., 2015. Optical properties of the urban aerosol particles obtained from ground based measurements and satellite-based modelling studies. *Adv. Meteorol.* 2015, 1–12. <https://doi.org/10.1155/2015/898376>.
- Myhre, G., Samset, B.H., Schulz, M., Balkanski, Y., Bauer, S., Bernsten, T.K., Zhou, C., 2013. Radiative forcing of the direct aerosol effect from AeroCom Phase II simulations. *Atmos. Chem. Phys.* 13 (4), 1853–1877. <https://doi.org/10.5194/acp-13-1853-2013>.
- Nomura, S., Mukai, H., Terao, Y., Takagi, K., Mohamad, M., Jahaya, M.F., 2018. Evaluation of forest CO<sub>2</sub> fluxes from sonde measurements in three different climatological areas including Borneo, Malaysia, and Iriomote and Hokkaido, Japan. *Tellus B* 70 (1), 1–19. <https://doi.org/10.1080/16000889.2018.1426316>.
- Pandolfi, M., Cusack, M., Alastuey, A., Querol, X., 2011. Variability of aerosol optical properties in the western mediterranean basin. *Atmos. Chem. Phys.* 11 (15), 8189–8203. <https://doi.org/10.5194/acp-11-8189-2011>.
- Petzold, A., Schönlinner, M., 2004. Multi-angle absorption photometry—a new method for the measurement of aerosol light absorption and atmospheric black carbon. *J. Aerosol Sci.* 35 (4), 421–441. <https://doi.org/10.1016/j.jaerosci.2003.09.005>.
- Petzold, A., Schloesser, H., Sheridan, P.J., Arnott, W.P., Ogren, J.A., Virkkula, A., 2005. Evaluation of multiangle absorption photometry for measuring aerosol light absorption. *Aerosol. Sci. Technol.* 39 (1), 40–51. <https://doi.org/10.1080/027868290901945>.
- Pyle, J.A., Warwick, N.J., Harris, N.R., Abas, M.R., Archibald, A.T., Ashfold, M.J., Young, P.J., 2011. The impact of local surface changes in Borneo on atmospheric composition at wider spatial scales: coastal processes, land-use change and air quality. *Philos. Trans. R. Soc. Lond. B Biol. Sci.* 366 (1582), 3210–3224. <https://doi.org/10.1098/rstb.2011.0060>.
- Ragsdale, K.M., Barrett, B.S., Testino, A.P., 2013. Variability of particulate matter (PM10) in Santiago, Chile by phase of the madden-julian oscillation (MJO). *Atmos. Environ.* 81, 304–310. <https://doi.org/10.1016/j.atmosenv.2013.09.011>.
- Rama Gopal, K., Balakrishnaiah, G., Arafath, S.M., Raja Obul Reddy, K., Siva Kumar Reddy, N., Pavan Kumari, S., Mallikarjuna Reddy, P., 2017. Measurements of scattering and absorption properties of surface aerosols at a semi-arid site, Anantapur. *Atmos. Res.* 183, 84–93. <https://doi.org/10.1016/j.atmosres.2016.08.016>.
- Ramage, C.S., 1968. Role of a tropical “maritime continent” in the atmospheric circulation. *Mon. Weather Rev.* 96, 365–370.
- Reddington, C.L., Yoshioka, M., Balasubramanian, R., Ridley, D., Toh, Y.Y., Arnold, S.R., Spracklen, D.V., 2014. Contribution of vegetation and peat fires to particulate air pollution in Southeast Asia. *Environ. Res. Lett.* 9, 1–12, 094006.
- Reid, J.S., Eck, T.F., Christopher, S.A., Koppmann, R., Dubovik, O., Eleuterio, D.P., Zhang, J., 2005. A review of biomass burning emissions part III: intensive optical properties of biomass burning particles. *Atmos. Chem. Phys.* 5, 827–849.
- Reid, J.S., Xian, P., Hyer, E.J., Flatau, M.K., Ramirez, E.M., Turk, F.J., Maloney, E.D., 2012. Multi-scale meteorological conceptual analysis of observed active fire hotspot activity and smoke optical depth in the Maritime Continent. *Atmos. Chem. Phys.* 12 (4), 2117–2147. <https://doi.org/10.5194/acp-12-2117-2012>.
- Reid, J.S., Hyer, E.J., Johnson, R.S., Holben, B.N., Yokelson, R.J., Zhang, J., Liew, S.C., 2013. Observing and understanding the Southeast Asian aerosol system by remote sensing: an initial review and analysis for the Seven Southeast Asian Studies (7SEAS) program. *Atmos. Res.* 122, 403–468. <https://doi.org/10.1016/j.atmosres.2012.06.005>.
- Reid, J.S., Lagrosas, N.D., Jonsson, H.H., Reid, E.A., Sessions, W.R., Simpkins, J.B., Zhang, J., 2015. Observations of the temporal variability in aerosol properties and their relationships to meteorology in the summer monsoonal South China Sea/East

- Sea: the scale-dependent role of monsoonal flows, the Madden-Julian Oscillation, tropical cyclones, squall lines and cold pools. *Atmos. Chem. Phys.* 15 (4), 1745–1768. <https://doi.org/10.5194/acp-15-1745-2015>.
- Reid, J.S., Xian, P., Holben, B.N., Hyer, E.J., Reid, E.A., Salinas, S.V., Zhang, C., 2016. Aerosol meteorology of the Maritime Continent for the 2012 7SEAS southwest monsoon intensive study – Part 1: regional-scale phenomena. *Atmos. Chem. Phys.* 16 (22), 14041–14056. <https://doi.org/10.5194/acp-16-14041-2016>.
- Reynolds, G., Payne, J., Sinun, W., Mosigil, G., Walsh, R.P., 2011. Changes in forest land use and management in Sabah, Malaysian Borneo, 1990–2010, with a focus on the Danum Valley region. *Philos. Trans. R. Soc. Lond. B Biol. Sci.* 366 (1582), 3168–3176. <https://doi.org/10.1098/rstb.2011.0154>.
- Rizzo, L.V., Artaxo, P., Müller, T., Wiedensohler, A., Paixão, M., Cirino, G.G., Kulmala, M., 2013. Long term measurements of aerosol optical properties at a primary forest site in Amazonia. *Atmos. Chem. Phys.* 13 (5), 2391–2413. <https://doi.org/10.5194/acp-13-2391-2013>.
- Roesch, A., Schmidbauer, H., 2018. WaveletComp: Computational Wavelet Analysis: R Package Version 1.1. Retrieved from. [https://www.researchgate.net/publication/323836523\\_WaveletComp\\_11\\_A\\_guided\\_tour\\_through\\_the\\_R\\_package](https://www.researchgate.net/publication/323836523_WaveletComp_11_A_guided_tour_through_the_R_package).
- Salinas, S.V., Chew, B.N., Liew, S.C., 2009. Retrievals of aerosol optical depth and Angstrom exponent from ground-based Sun-photometer data of Singapore. *Appl. Opt.* 48 (8), 1473–1484. <https://doi.org/10.1364/ao.48.001473>.
- Samset, B.H., Stjern, C.W., Andrews, E., Kahn, R.A., Myhre, G., Schulz, M., Schuster, G.L., 2018. Aerosol absorption: progress towards global and regional constraints. *Curr. Clim. Change Rep.* 4 (2), 65–83. <https://doi.org/10.1007/s40641-018-0091-4>.
- Schuster, G.L., Dubovik, O., Holben, B.N., 2006. Angstrom exponent and bimodal aerosol size distributions. *J. Geophys. Res.* 111 (D7) <https://doi.org/10.1029/2005jd006328>.
- Shindell, D., Faluvegi, G., 2009. Climate response to regional radiative forcing during the twentieth century. *Nat. Geosci.* 2 (4), 294–300. <https://doi.org/10.1038/ngeo473>.
- Sun, T., Che, H., Qi, B., Wang, Y., Dong, Y., Xia, X., Zhang, X., 2018. Aerosol optical characteristics and their vertical distributions under enhanced haze pollution events: effect of the regional transport of different aerosol types over eastern China. *Atmos. Chem. Phys.* 18 (4), 2949–2971. <https://doi.org/10.5194/acp-18-2949-2018>.
- Tan, F., Lim, H.S., Abdullah, K., Yoon, T.L., Holben, B., 2015. AERONET data-based determination of aerosol types. *Atmos. Pollut. Res.* 6 (4), 682–695. <https://doi.org/10.5094/apr.2015.077>.
- Tian, B., Waliser, D.E., Kahn, R.A., Li, Q., Yung, Y.L., Tyranowski, T., Smirnov, A., 2008. Does the Madden-Julian Oscillation influence aerosol variability? *J. Geophys. Res.* 113 (D12) <https://doi.org/10.1029/2007jd009372>.
- Torrence, C., Compo, G.P., 1998. A practical guide to wavelet analysis. *Bull. Am. Meteorol. Soc.* 79, 61–78.
- Wang, J., Ge, C., Yang, Z., Hyer, E.J., Reid, J.S., Chew, B.-N., Zhang, M., 2013. Mesoscale modeling of smoke transport over the Southeast Asian Maritime Continent: interplay of sea breeze, trade wind, typhoon, and topography. *Atmos. Res.* 122, 486–503. <https://doi.org/10.1016/j.atmosres.2012.05.009>.
- Wang, J., Lu, X., Yan, Y., Zhou, L., Ma, W., 2020. Spatiotemporal characteristics of PM2.5 concentration in the Yangtze River Delta urban agglomeration, China on the application of big data and wavelet analysis. *Sci. Total Environ.* 724, 138134. <https://doi.org/10.1016/j.scitotenv.2020.138134>.
- Wen, M., Zhang, R., 2008. Quasi-biweekly oscillation of the convection around Sumatra and low-level tropical circulation in Boreal spring. *Mon. Weather Rev.* 136 (1), 189–205. <https://doi.org/10.1175/2007mwr1991.1>.
- Xin, J., Gong, C., Wang, S., Wang, Y., 2016. Aerosol direct radiative forcing in desert and semi-desert regions of northwestern China. *Atmos. Res.* 171, 56–65. <https://doi.org/10.1016/j.atmosres.2015.12.004>.
- Yin, S., 2020. Biomass burning spatiotemporal variations over south and Southeast Asia. *Environ. Int.* 145, 106153. <https://doi.org/10.1016/j.envint.2020.106153>.
- Zhao, H., Che, H., Ma, Y., Xia, X., Wang, Y., Wang, P., Wu, X., 2015. Temporal variability of the visibility, particulate matter mass concentration and aerosol optical properties over an urban site in Northeast China. *Atmos. Res.* 166, 204–212. <https://doi.org/10.1016/j.atmosres.2015.07.003>.